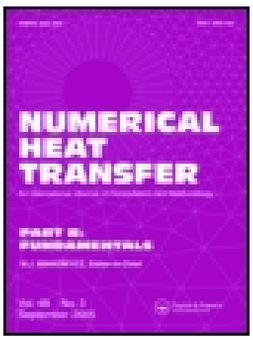

Numerical Heat Transfer: Part B: Fundamentals

ISSN: 1040-7790 (Print) 1521-0626 (Online) Journal homepage: https://www.tandfonline.com/loi/unhb20

LATTICE BOLTZMANN METHOD FOR THE HEAT CONDUCTION PROBLEM WITH PHASE CHANGE

Wen-Shu Jiaung, Jeng-Rong Ho, Chun-Pao Kuo

To cite this article: Wen-Shu Jiaung, Jeng-Rong Ho, Chun-Pao Kuo (2001) LATTICE BOLTZMANN METHOD FOR THE HEAT CONDUCTION PROBLEM WITH PHASE CHANGE, Numerical Heat Transfer: Part B: Fundamentals, 39:2, 167-187, DOI: 10.1080/10407790150503495

To link to this article: https://doi.org/10.1080/10407790150503495

Numerical Heat Transfer, Part B, 39:167–187, 2001

1040-7790/01 $12.00 + .00

LATTICE BOLTZMANN METHOD FOR THE HEAT CONDUCTION PROBLEM WITH PHASE CHANGE

Wen-Shu Jiaung, Jeng-Rong Ho, and Chun-Pao Kuo
Department of Mechanical Engineering, National Chung Cheng University, Chia-Yi, Taiwan 621, Republic of China

An extended lattice Boltzmann (LB) equation was developed for the simulation of the phase-change problem governed by the heat conduction equation incorporated with enthalpy formation. Mathematical consistency between the proposed extended LB equation and the governing equation was accomplished by the Chapman-Enskog expansion. Illustrative examples include one-dimensional half-space melting and solidification as well as two-dimensional solidification in a corner. Phase change at a single temperature and with a mushy zone are both demonstrated. Two types of boundary condition, prescribed temperature and prescribed heat flux, are considered in the illustrative examples. Different thermal diffusivities in the separated phases/zones are accomplished through varying the relaxation times in the LB equation. All numerical results obtained by the present scheme agree very well with previous analytical or numerical results in the literature.

INTRODUCTION

The transient heat conduction problem involving a change of phase is of particular interest in many engineering problems, such as the casting of metals, melting and solidification of alloys, artificial crystal growth from melts, and storage of energy. Due to the inherent nonlinearities, mainly caused by formation and propagation of the moving phase-change interface, the analytical solutions to these problems are limited to problems with simple geometry and boundary conditions [1–3]. Numerical methods are, therefore, more frequently employed in solving such phase-change problems and have led to impressive results [4–10].

To date, mathematical modeling of the phase-change problem has been based mostly on continuum approaches. Recently the lattice Boltzmann (LB) method has been developed as a powerful tool for the solution of partial differential equations [11–21]. This method is derived from the lattice gas automata (LGA) method and inherits from the LGA some of its major advantages over conventional computational methods. The LB method simulates physical transport phenomena

Received 31 July 2000; revised 25 September 2000.

Support for this work by the National Science Counsel of the Republic of China under Grant NSC89-2212-E-194-015 is gratefully acknowledged.

Address correspondence to Prof. J.-R. Ho, Department of Mechanical Engineering, National Chung Cheng University, 160, San-Hsing, Ming-Hsiung, Chia-Yi 621, Taiwan, Republic of China. E-mail: imejrho@ccunix.ccu.edu.tw

NOMENCLATURE

b	number of propagation directions in a lattice
C	specific heat at constant pressure
e	propagation speed ($=\Delta x/\Delta t$)
$\mathbf{e}_i$	propagation velocity in the direction i in a lattice
f_l	volume phase fraction of the liquid phase
H	total enthalpy
k	thermal conductivity
L	latent heat of phase change
$M(t)$	interfacial position as a function of time, t
n_i	particle distribution function in the i direction
$n_i^{(0)}$	equilibrium particle distribution function in the i direction
O	order of magnitude
q	heat flux
St	Stefan number
t	time
T	temperature
T_i	initial temperature
T_m	melting temperature
T_0	temperature on boundary at $x=0$
w_i	weight factor in the i direction
x,y	axial coordinate
Y	characteristic length
α	thermal diffusivity
ϵ	small quantity for Chapman-Enskog expansion
ρ	density
σ	phase-change interval
τ	relaxation time
Δx	lattice size
Δt	time step
Φ	source term

Superscripts

k	iteration index
*	dimensionless variable
(1)	$O(\epsilon)$ in the Chapman-Enskog expansion
(2)	$O(\epsilon^2)$ in the Chapman-Enskog expansion

Subscripts

0	lattice center or location at $x=0$
i	direction i in a lattice
j	lattice index
l	liquid phase
m	mushy zone
s	solid phase
sm	interface between the solid phase and the mushy zone
ml	interface between the mushy zone and the liquid phase

with quasi-particles populating lattices. The quasi-particles propagate across the lattice along links connecting neighboring lattice sites, and the particles then undergo collisions upon arrival at a lattice site. For simulating physical phenomena, the collisions among particles must obey suitable physical laws. Thus, the fundamental idea of the LB method is to construct simplified kinetic models that incorporate the essential physics of microscopic processes so that the macroscopic averaged properties obey the desired laws. Generally, the LB method has some attractive properties, such as its simple implementation on a computer, ability to handle complex geometry and boundary conditions, capability of stable and accurate simulation, as well as the inherent parallel nature. More detailed descriptions of the LB method are given in the review article by Chen and Doolen [16] and the recently published book by Wolf-Gladrow [17].

In the application of the LB method to the heat conduction problem, Wolf-Gladrow [18] first derived the LB equation for diffusion. In his study, the resulting algorithm with a relaxation parameter of unity was identical to an explicit finite-difference formulation at its stability limit. The time step of the explicit LB equation was limited by accuracy, not by stability requirements. De Fabritiis and co-workers [19] proposed a generalized mesoscopic LB model for describing

flows with solid/liquid phase transitions. The phase transition was represented by a chemical term, while the melting and solidification were analogous to exothermic and endothermic chemical reactions, respectively. Their model was also suitable to describe chaotic motions in the mushy zone. van der Sman and co-workers [20] developed a LB scheme for simulation of the heat and mass transfer during cooling of packed cut flowers. Their one-dimensional convection-diffusion scheme had second-order accuracy and showed low numerical diffusion even at high Peclet and Courant numbers.

The above literature review indicates that the LB method is a suitable method for multiple-phase problems. To the authors' best knowledge, no works on the LB method for the heat conduction equation with phase change have been presented. In the present study, a complete heat conduction equation with phase change is first introduced with enthalpy formulation in which the interfacial position of phase change can be determined through the liquid-phase fraction. Subsequently, the discretized, extended LB equation with BGK approximation is introduced. Then, Chapman-Enskog expansion is employed to demonstrate that the proposed extended LB equation macroscopically matches the governing equation. What follows is the presentation of the numerical solution procedure that incorporates the enthalpy formulation into the extended LB equation as well as implementation of boundary condition. Finally, several illustrative examples are simulated and results obtained by the present scheme are compared with previous analytical or numerical solutions.

ENTHALPY FORMULATION FOR PHASE CHANGE

In the enthalpy formulation approach, the energy equation is initially expressed in terms of the total enthalpy. The governing equation for a heat conduction problem can thus be cast in the form

$$\frac{\partial(\rho H)}{\partial t} = \nabla \cdot (k \nabla T) \tag{1}$$

The total enthalpy, H, is further split into the sensible enthalpy and the latent heat for the phase-change problem [4]. In this manner, the phase boundary can be solved naturally and determined as part of the solution [5]. H can be written as

$$H = CT + f_l L \tag{2}$$

where C and L represent the constant-pressure specific heat and the latent heat of phase change; f_l is the volume-phase fraction of the liquid phase and is zero for the solid region and unity for the liquid region. The phase fraction lies between zero and unity when the region being considered is undergoing phase change. Substituting Eq. (2) into Eq. (1) yields

$$\frac{\partial(\rho C T)}{\partial t} = \nabla \cdot (k \nabla T) - L \frac{\partial(\rho f_l)}{\partial t} \tag{3}$$

where the latent heat appears as a heat source term in the governing equation. If the density ρ and the specific heat C are explicitly independent of time, and the thermal

conductivity k is independent of position, Eq. (3) can be written as

$$\frac{\partial T}{\partial t} = \alpha \nabla^2 T - \frac{L}{C}\frac{\partial f_l}{\partial t} \tag{4}$$

To complete the physical model described by Eq. (4), the so-called H-based method [5] is employed to determine the relationship between the liquid fraction and temperature. First the relationship between T and H is established as

$$T = \begin{cases} \dfrac{H}{C} & H < H_s \\ T_s + \left(\dfrac{2\sigma}{L + 2C\sigma}\right)(H - H_s) & H_s \le H \le H_l \\ \dfrac{H - L}{C} & H > H_l \end{cases} \tag{5}$$

where H_s and H_l are the enthalpy values corresponding, respectively, to the T_s and T_l temperatures, in which T_s and T_l represent the temperatures at the beginning and end of a phase change (melting), respectively; σ is the phase-change interval, and its value is zero for a pure substance undergoing isothermal phase change. Once the enthalpy is determined, the liquid phase fraction is then defined as

$$f_l = \frac{H - H_s}{H_l - H_s} \tag{6}$$

Equations (4)–(6) form a complete set of equations for modeling a heat conduction problem with phase change. More detailed descriptions and advantages regarding this model can be found in [5].

THE LATTICE BOLTZMANN METHOD FOR HEAT CONDUCTION EQUATION WITH PHASE CHANGE

The lattice Boltzmann (LB) method is a discrete, in space and time, kinetic equation description for the evolution of the particle distribution of a lattice gas whose density represents the physical quantities to be modeled, such as temperature. In this section, first the discretized, extended LB equation with BGK approximation is described. Subsequently, the consistence between the extended LB equation and the heat conduction equation with phase change is analyzed by the Chapman-Enskog expansion. The solution procedure to the LB equation is then described, and finally, the implementation of initial and boundary conditions are discussed.

BGK Lattice Boltzmann Model

The starting point of the LB method is the kinetic equation for the particle distribution function, $n_i(\mathbf{x}, t)$:

$$\frac{\partial n_i(\mathbf{x}, t)}{\partial t} + \mathbf{e}_i \cdot \nabla n_i(\mathbf{x}, t) = \Omega_i \qquad i = 0, 1, 2, \ldots, b \tag{7}$$

where n_i is the particle distribution functions denoting the number of particles at

lattice node $\boldsymbol{x}$ and time t, moving in direction i with velocity $\boldsymbol{e_i}$ along the lattice link $\Delta \boldsymbol{x_i} = \boldsymbol{e_i}\Delta \boldsymbol{t}$ connecting nearest neighbors. The term Ω_i represents the rate of change of n_i due to collisions. The discrete Boltzmann equation, Eq. (7), with BGK approximation [14, 17] reads

$$\frac{\partial n_i(\mathbf{x}, t)}{\partial t} + \mathbf{e}_i \cdot \nabla n(\mathbf{x}, t) = -\frac{1}{\tau}\left[n_i(\mathbf{x}, t) - n_i^{(0)}(\mathbf{x}, t)\right] \tag{8}$$

Here collisions are modeled as a relaxation with relaxation time τ toward an equilibrium distribution $n_i^{(0)}$. A discretization equation of Eq. (8) is given by

$$\frac{n_i(\mathbf{x}, t+\Delta t) - n_i(\mathbf{x}, t)}{\Delta t} + \mathbf{e}_i \cdot \frac{n_i(\mathbf{x} + \mathbf{e}_i \Delta t, t + \Delta t) - n_i(\mathbf{x}, t + \Delta t)}{\mathbf{e}_i \, \Delta t}$$
$$= -\frac{1}{\tau}\left[n_i(\mathbf{x}, t) - n_i^{(0)}(\mathbf{x}, t)\right]$$

After canceling two terms of $n_i(\boldsymbol{x}, t + \Delta t)$ on the left-hand side, the equation becomes

$$n_i(\mathbf{x} + \mathbf{e}_i \Delta t, \ t + \Delta t) - n_i(\mathbf{x}, t) = -\frac{\Delta t}{\tau}\left[n_i(\mathbf{x}, t) - n_i^{(0)}(\mathbf{x}, t)\right] \tag{9}$$

This is the LB equation with BGK approximation that describes the evolution of the particle distribution n_i. For the heat conduction equation the temperature is obtained after summing n_i over all directions, i.e.,

$$T(\mathbf{x}, t) = \sum_{i=0}^{b} n_i(\mathbf{x}, t) \tag{10}$$

An equilibrium distribution is required to continue to process Eq. (9). For the heat conduction problem, it can be simply chosen as

$$n_i^{(0)}(\mathbf{x}, t) = w_i T(\mathbf{x}, t) \tag{11}$$

Here w_i represents the weight factors in the direction i, whose values for the one-dimensional D1Q2 lattice and two-dimensional D2Q9 lattice are given in Figure 1.

The weight factors satisfy the relation: $\sum_{i=0}^{b} w_i = 1$, and the distribution functions $n_i^{(0)}(\mathbf{x}, t)$ and $n_i^{(1)}(\mathbf{x}, t)$ satisfy the following two equations:

$$\sum_{i=0}^{b} n_i^{(0)}(\mathbf{x}, t) = \sum_{i=0}^{b} w_i T(\mathbf{x}, t) = T(\mathbf{x}, t) \tag{12}$$

and

$$\sum_{i=0}^{b} n_i^{(1)}(\mathbf{x}, t) = 0 \tag{13}$$

By analogy with the source term in Eq. (4), a source term is introduced to the LB equation, Eq. (9). Thus, the proposed, extended LB equation reads as

$$n_i(\mathbf{x} + \mathbf{e}_i \Delta t, t + \Delta t) - n_i(\mathbf{x}, t) = -\frac{\Delta t}{\tau}\left[n_i(\mathbf{x}, t) - n_i^{(0)}(\mathbf{x}, t)\right] - \Delta t \, \Phi_i \tag{14}$$

where Φ_i represents the source which affects the distribution function n_i and comes

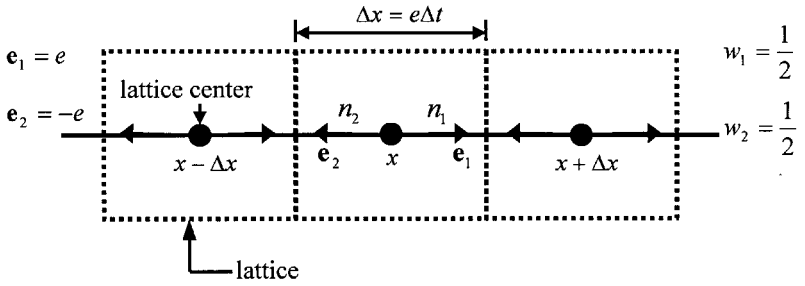

(a)

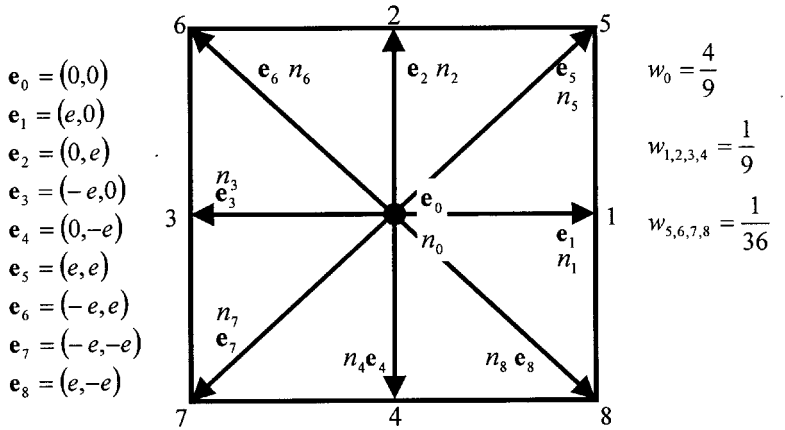

(b)

Figure 1. Schematic diagrams showing (*a*) one-dimensional D1Q2 lattice and (*b*) two-dimensional D2Q9 lattice. Two velocities, $\mathbf{e}_1$ and $\mathbf{e}_2$, are used for the D1Q2 lattice, and nine velocities, $\mathbf{e}_0$ to $\mathbf{e}_8$, are used for the D2Q9 lattice. Values of the weighting factors, w_i, are also given.

from the direction i in a lattice. Φ_i is taken as

$$\Phi_i = w_i \Phi \tag{15}$$

Chapman-Enskog Expansion

The Chapman-Enskog expansion has already been used to derive the Euler, Navier-Stokes, and other macroscopic equations for LB models [12–15, 20, 21].

The essential spirits of the Chapman-Enskog expansion are to reveal the macroscopic behavior of the LB equation deviating from the equilibrium distribution when disturbed by a small perturbation [22, 23]. In the Chapman-Enskog expansion the particle distribution functions, n_i, are expanded up to linear terms in the expansion parameter ε:

$$n_i = n_i^{(0)} + \varepsilon n_i^{(1)} + O(\varepsilon^2) \tag{16}$$

where ε is a small quantity, i.e., $|\varepsilon| \ll 1$. Since the fundamental transfer mechanism for heat conduction is diffusion, which is a slow process on large spatial scales, that suggests the following scaling [18, 22]:

$$\begin{aligned} \partial_t &\approx \varepsilon^2 \partial_{t^{(2)}} \\ \partial_{\mathbf{x}} &\approx \varepsilon \partial_{\mathbf{x}^{(1)}} \end{aligned} \tag{17}$$

where $t^{(2)}$ is the slow time scale associated with the diffusive process and $\boldsymbol{x}^{(1)}$ represent the corresponding relative large spatial scale. The expansion of $n_i(\mathbf{x} + \mathbf{e}_i\,\Delta t,\ t + \Delta t)$ is given as

$$\begin{aligned} n_i(\mathbf{x} + \mathbf{e}_i \Delta t,\ t + \Delta t) = n_i(\mathbf{x}, t) + \Delta t \partial_t n_i + \Delta t \partial_{x_\alpha} e_{i\alpha} n_i \\ + \frac{1}{2}(\Delta t)^2 \left(\partial_t \partial_t n_i + 2\partial_t \partial_{x_\alpha} e_{i\alpha} n_i + \partial_{x_\alpha} \partial_{x_\beta} e_{i\alpha} e_{i\beta} n_i \right) + O(\Delta t^3) \end{aligned} \tag{18}$$

Substituting Eq. (18) into Eq. (14) and expressing in terms of new scales suggested by Eq. (17) yields

$$\begin{aligned} \varepsilon^2 \partial_{t^{(2)}} n_i + \varepsilon \partial_{x_\alpha^{(1)}} e_{i\alpha} n_i + \frac{1}{2}\,\Delta t\, \varepsilon^2 \partial_{x_\alpha^{(1)}} \partial_{x_\beta^{(1)}} e_{i\alpha} e_{i\beta} n_i \\ = -\frac{1}{\tau}(n_i - n_i^{(0)}) - \Phi_i + O(\Delta t^2) + O(\varepsilon^3) \end{aligned} \tag{19}$$

In Eq. (16), terms with order of magnitude larger than $O(\varepsilon^3)$ are truncated. To recover Eq. (4), summation over all states for Eq. (19) is given as

$$\begin{aligned} \sum_i \varepsilon^2 \partial_{t^{(2)}} n_i + \sum_i \varepsilon \partial_{x_\alpha^{(1)}}\, e_{i\alpha} n_i + \frac{1}{2}\,\Delta t \sum_i \varepsilon^2 \partial_{x_\alpha^{(1)}} \partial_{x_\beta^{(1)}} e_{i\alpha} e_{i\beta} n_i \\ = -\frac{1}{\tau} \sum_i (n_i - n_i^{(0)}) - \sum_i \Phi_i + O(\Delta t^2) + O(\varepsilon^3) \end{aligned} \tag{20}$$

The first term on the LHS of Eq. (20) corresponds to the unsteady term as

$$\sum_i \varepsilon^2 \partial_{t^{(2)}} n_i = \sum_i \partial_t n_i = \partial_t T$$

The second term on the LHS of Eq. (20) is derived as

$$\begin{aligned}\sum_i \varepsilon\partial_{x_\alpha^{(1)}} e_{i\alpha} n_i &= \sum_i \varepsilon\partial_{x_\alpha^{(1)}} e_{i\alpha}\left[n_i^{(0)} + \varepsilon n_i^{(1)} + O(\varepsilon^2)\right] + O(\varepsilon^3)\\ &= \varepsilon\partial_{x_\alpha^{(1)}} \sum_i e_{i\alpha} n_i^{(0)} + \varepsilon^2 \partial_{x_\alpha^{(1)}} \sum_i e_{i\alpha} n_i^{(1)} + O(\varepsilon^3)\\ &= \varepsilon\partial_{x_\alpha^{(1)}} \sum_i e_{i\alpha}\left(-\tau\varepsilon\partial_{x_\beta^{(1)}} e_{i\beta} n_i^{(0)}\right) = -\tau\varepsilon^2 \partial_{x_\alpha^{(1)}}\partial_{x_\beta^{(1)}} e_{i\alpha} e_{i\beta} n_i^{(0)}\\ &= \begin{cases} -\tau e^2 \nabla^2 T & \text{(for D1Q2 lattice)}\\ -\dfrac{\tau}{3} e^2 \nabla^2 T & \text{(for D2Q9 lattice)}\end{cases}\end{aligned}$$

The third term on the LHS of Eq. (20) becomes

$$\frac{1}{2}\Delta t \sum_i \varepsilon^2 \partial_{x_\alpha^{(1)}}\partial_{x_\beta^{(1)}} e_{i\alpha} e_{i\beta} n_i = \frac{1}{2}\Delta t \sum_i \varepsilon^2 \partial_{x_\alpha^{(1)}}\partial_{x_\beta^{(1)}} e_{i\alpha} e_{i\beta}\left[n_i^{(0)} + \varepsilon n_i^{(1)} + O(\varepsilon^2)\right]$$

$$= \frac{1}{2}\Delta t \varepsilon^2 \partial_{x_\alpha^{(1)}}\partial_{x_\beta^{(1)}} \sum_i e_{i\alpha} e_{i\beta} n_i^{(0)} + O(\varepsilon^3) = \begin{cases} \dfrac{\Delta t}{2} e^2 \nabla^2 T & \text{(for D1Q2 lattice)}\\ \dfrac{\Delta t}{6} e^2 \nabla^2 T & \text{(for D2Q9 lattice)}\end{cases}$$

The RHS of Eq. (20) is given as

$$-\frac{1}{\tau}\left(\sum_i n_i - \sum_i n_i^{(0)}\right) - \sum_i \Phi_i = -\frac{1}{\tau}(T - T) - \Phi = -\Phi$$

Thus, Eq. (20) becomes

$$\frac{\partial T}{\partial t} = \begin{cases} \dfrac{e^2}{2}(2\tau - \Delta t)\nabla^2 T - \Phi & \text{(for D1Q2 lattice)}\\ \dfrac{e^2}{6}(2\tau - \Delta t)\nabla^2 T - \Phi & \text{(for D2Q9 lattice)}\end{cases} \tag{21}$$

Equation (4) is recovered as long as α is chosen as $(e^2/2)(2\tau - \Delta t)$ for the D1Q2 lattice and $(e^2/6)(2\tau - \Delta t)$ for the D2Q9 lattice, and Φ is set to be

$$\frac{L}{C}\frac{\partial f_l}{\partial t}$$

Numerical Solution Procedure

The evolution law for the particle distribution function $n_i(\mathbf{x}, t)$ is governed by the extended LB equation described by Eq. (14), which can be rewritten as

$$n_i(\mathbf{x} + \mathbf{e}_i\,\Delta t,\ t + \Delta t) = n_i(\mathbf{x}, t) + \Delta_i[n_i(\mathbf{x}, t)] - \Delta t\,\Phi_i \tag{22}$$

where

$$\Delta_i = -\frac{\Delta t}{\tau}\left[n_i(\mathbf{x}, t) - n_i^{(0)}(\mathbf{x}, t)\right]$$

In a typical simulation the initial temperature distribution $T(\mathbf{x}, 0)$ and the liquid-phase fraction, f_l, are given as initial conditions. The initial distribution function $n_i(\mathbf{x}, 0)$ are calculated using one term in the expansion expression, Eq. (16). That is, $n_i(\mathbf{x}, 0)$ was set to be $n_i^{(0)}(\mathbf{x}, 0)$, which depends only on the initial temperature. Distribution functions are then evolved according to Eq. (22). It is noted that the initial disturbances can be introduced through boundary lattices even if the initial liquid-phase fraction is zero.

During each marching time step the iterative procedures for the nonlinear term were executed as follows.

1. The kth iteration value at the new time level $t + \Delta t$ for the particle distribution function is evaluated according to Eq. (22) as

$$n_i^k(\mathbf{x} + \mathbf{e}_i\,\Delta t,\ t + \Delta t) = n_i(\mathbf{x}, t) + \Delta_i[n_i(\mathbf{x}, t)] - \Delta t\, w_i \frac{L}{C}\left[\frac{f_{l,i}^{k-1}(t + \Delta t) - f_{l,i}(t)}{\Delta t}\right] \tag{23}$$

   where the superscripts k and $k-1$ represent the current and previous iteration levels, respectively.
2. Temperatures at the kth iteration level are then calculated according to Eq. (10).
3. The total enthalpies at the kth iteration level are then calculated as

$$H^k = CT^k + f_l^{k-1}L$$

4. The liquid-phase fractions at the current iteration level are then updated:

$$f_l^k = \begin{cases} 0 & H^k < H_s \\ \dfrac{H^k - H_s}{H_l - H_s} & H_s \le H^k \le H_l \\ 1 & H^k > H_l \end{cases}$$

5. The f_l^k obtained values are then used for the next iteration level $k + 1$, that is, steps 1–4 are repeated until the following convergence criterion is satisfied:

$$\min\left(\left|\frac{f_l^k - f_l^{k-1}}{f_l^{k-1}}\right|,\ \left|\frac{T^k - T^{k-1}}{T^K}\right|\right) < 10^{-8}$$

Boundary Conditions

In the LB method, boundary condition is usually implemented conveniently and naturally through the particle fluxes crossing the boundary lattice cells. Two

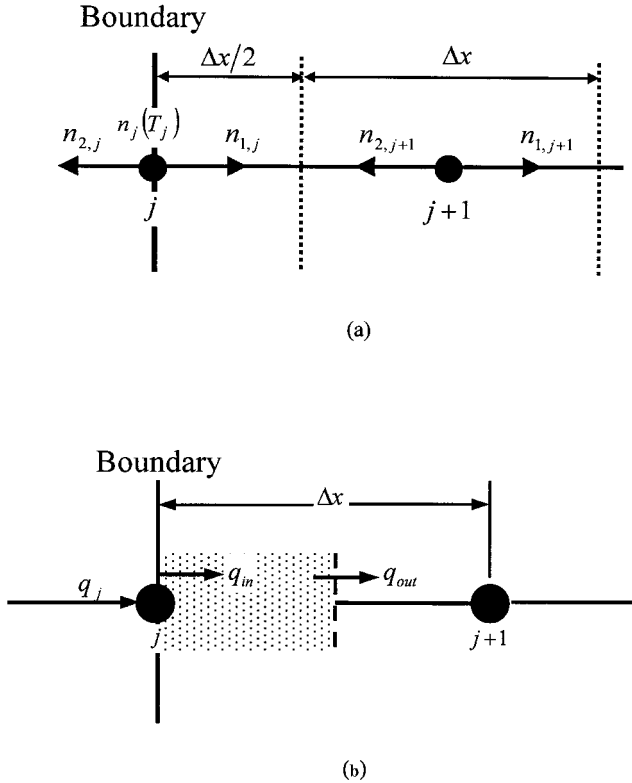

Figure 2. Schematic diagram for illustrating implementation of boundary condition on the boundary lattice j. (*a*) The distribution function $n_j(T_j)$ is fixed if the temperature on the boundary is at T_j. (*b*) The half-sized lattice on which the conservation of energy is applied.

kinds of boundary condition are studied in the illustrative examples: prescribed temperature and prescribed heat flux. The prescribed temperature can be imposed by fixing the number density on the boundary [24, 25]. Without losing generality, the one-dimensional lattice is used to discuss this boundary condition. If a prescribed temperature T is set at the boundary lattice j, referring to Figure 2*a*, the equilibrium distribution function $n_j(T)$ is fixed. The distribution function $n_{1,j}$ (propagation in the $\mathbf{e}_i$ direction) can then be determined by

$$n_{1,j} = w_1 n_j(T) + w_2 n_j(T) - n_{2,j}$$

where $n_{2,j}$ represents the particle fluxes from the adjacent cell $j+1$ that can be obtained from the kinetic equation, Eq. (14).

For implementation of the prescribed heat flux, the conventional finite-volume method [26] can be used. First the conservation of energy is applied to the half-sized

boundary lattice j, referring to Figure 2b, as

$$\rho c \int_j^{j+1/2} \int_t^{t+\Delta t} \frac{\partial T}{\partial t} = \int_t^{t+\Delta t} (q_{\text{in}} - q_{\text{out}})\, dt \tag{24}$$

where material properties are assumed to be constants. The q_{in} in Eq. (24) represents the inlet heat flux and in equal to the prescribed heat flux q_j. The q_{out} denotes the heat flux leaving the control volume that can be described through Fourier's law. Thus Eq. (24) is approximated as

$$\rho c \frac{\Delta x}{2}(T_j^{n+1} - T_j^n) = \int_t^{t+\Delta t} \left[q_j - \frac{k(T_j - T_{j+1})}{\Delta x} \right] dt \tag{25}$$

The superscripts $n+1$ and n represent time levels evaluated at $t+\Delta t$ and t, respectively. For simplicity, an explicit scheme for time is employed in Eq. (25) and the following linear algebraic expression is derived:

$$a_j T_j^{n+1} = (a_j - a_{j+1}) T_j^n + a_{j+1} T_{j+1}^n + q_j \tag{26}$$

where $a_j = \rho c \Delta x / 2\Delta t$ and $a_{j+1} = k/\Delta x$. Equation (26) denotes that the temperature on the boundary can be expressed in terms of the heat flux. Thus, the prescribed heat flux can be proceeded as the wall temperature is prescribed.

RESULTS AND DISCUSSION

To demonstrate the feasibility and accuracy of the present numerical scheme, some test examples whose analytical or numerical solutions are available were performed. In this study, the numerical value of the time step Δt was set to be equal to the lattice size Δx and all computations were performed on a Pentium II 350 personal computer.

Example 1: Melting in a Half-Space (One-Region Problem)

In this example, a semi-infinite system subjected to two kinds of boundary condition, prescribed temperature and prescribed heat flux, was considered. Initially the full solid was at the phase-change temperature T_m, which was scaled to be zero. For the prescribed-temperature case, the temperature at $x = 0$ was suddenly raised to $T_0 = 1$ at time $t = 0$ and maintained at that temperature for all times $t > 0$. The prescribed-heat-flux case was accomplished by imposing a time-varying heat flux $\partial T/\partial x = -e^t$ at $x = 0$ for $t \geq 0$. The schematic diagram showing these two kinds of boundary condition, coordinates, and nomenclature is given in Figure 3. Once the boundary condition was imposed, melting began at the surface $x = 0$ and proceeded into the solid as the discrete liquid/solid interface moved in the positive x direction. This problem is a one-region problem because the solid phase is at a constant temperature throughout. The temperature is only unknown in the liquid phase [1].

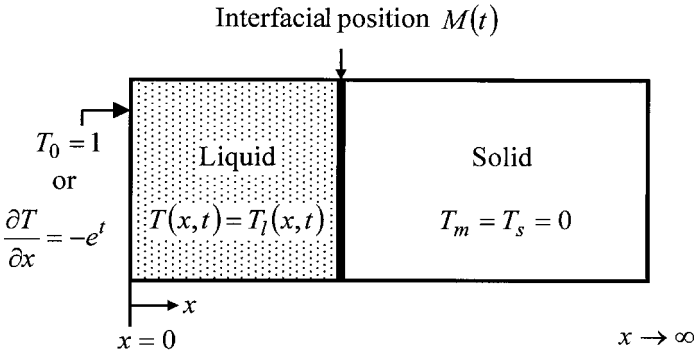

Figure 3. Schematic diagram showing the coordinate, nomenclature, boundary conditions, solid and liquid phases, and interfacial position for Example 1.

For the prescribed-temperature case, the solution was determined analytically in [1]. The temperature distribution has the form

$$T(x, t) = 1 - \frac{\operatorname{erfc}\left|x/2\sqrt{\alpha_l t}\right|}{\operatorname{erfc}(\lambda)}$$

and the liquid–solid interface as a function of time is given as

$$M(t) = 2\lambda\sqrt{\alpha_l t}$$

where λ are solutions to the transcendental equation $\lambda e^{\lambda^2} \operatorname{erfc}(\lambda) = \mathrm{St}/\sqrt{\pi}$. The Stefan number, St, is defined as $\mathrm{St} = \rho C_s(T_0 - T_m)/L$. The interfacial position as a function of time and the temperature distribution for different values of St and λ are presented in Figures 4 and 5.

The following numerical values, $\mathrm{St} = 0.1303$, $\lambda = 0.25$, $\alpha_l = 0.0025$, and $\tau = 1.0$, were set for computations in Figure 4 and 400 lattices in total were used in the computational range from $x = 0$ to 1. The interfacial position as a function of time and the temperature distribution as a function of position at different times are shown in Figures 4*a* and 4*b*, respectively. Excellent agreement between the analytical solution and the present solution is shown in Figure 4. In Figure 5, our numerical scheme was further tested by a higher St number up to 2.8576, which implies the interface of phase change moving with a much faster speed. Again, excellent agreement between the present result and the analytical solution is shown. The relative error in numerical value is less than 1%.

For the prescribed-heat-flux case, the analytical solution to the problem was given by Furzeland [27] as $T(x, t) = e^{t-x}$ and $M(t) = t$ for $\mathrm{St} = 1$. Figure 6 shows the temperature distribution as a function of position at $t = 0.5$, 1, 1.5, and 2. There were 150 lattices uniformly distributed in the computational range from $x^* = 0$ to 3. The thermal diffusivity and relaxation time were both set to be unity. Again our numerical results coincide closely with the analytical solutions.

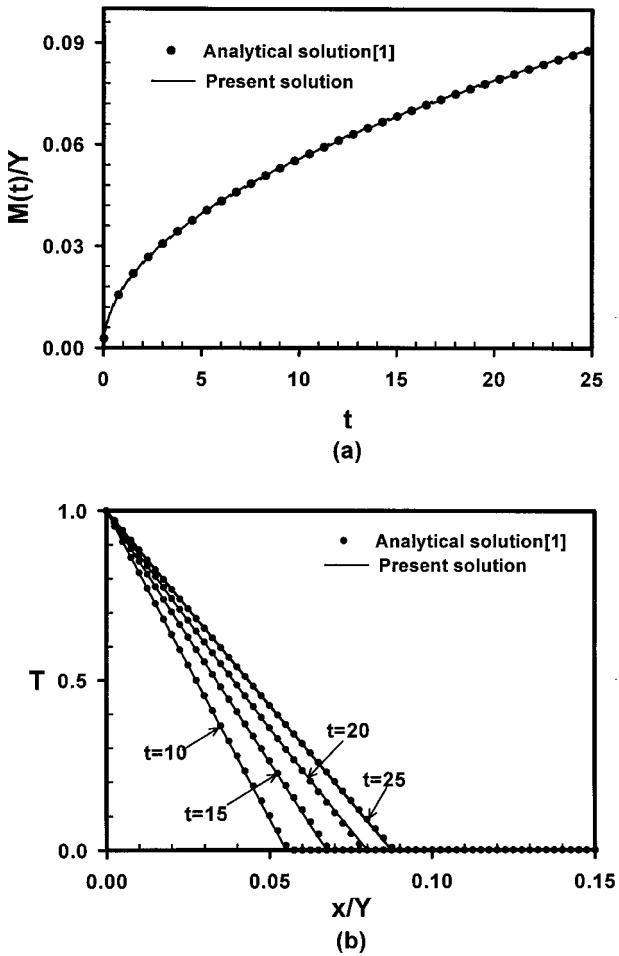

Figure 4. Panels showing the comparison between present computational solutions and analytical solutions for Example 1 (St = 0.1303). Interfacial position as a function of time and temperature distribution as a function of position at different times are shown in (*a*) and (*b*), respectively.

The close agreeemnt our solutions and the analytical solutions shows that the proposed LB schemes can precisely predict the melting problem with constant properties.

Example 2: Solidification in a Half-Space (Two-Region Problem)

In this example, the half-space solidification problem was considered. Initially the system was at a uniform liquid temperature $T = T_i = 2$ that was higher than the melting temperature $T_m = 1$. At time $t = 0$ the boundary surface at $x = 0$ was lowered to a temperature $T_0 = 0$ and kept at that temperature for all times $t > 0$. Since the solidification starts at the surface $x = 0$, the solid–liquid interface moves in the positive x direction. The schematic diagram for this problem is given in Figure 7. This is a two-region problem because temperatures in the solid and liquid phases are unknown [1]. The analytical solutions for temperature distribution in the solid

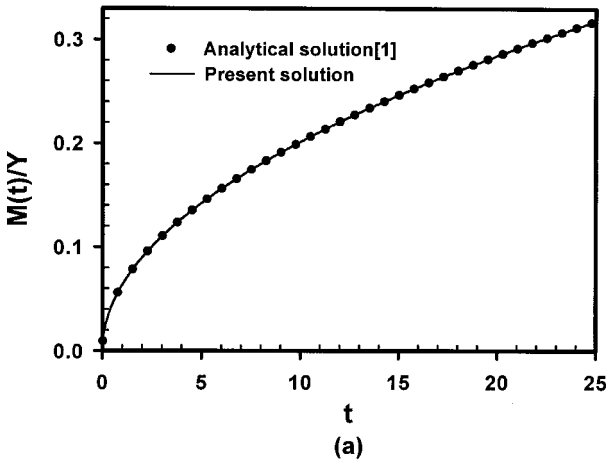

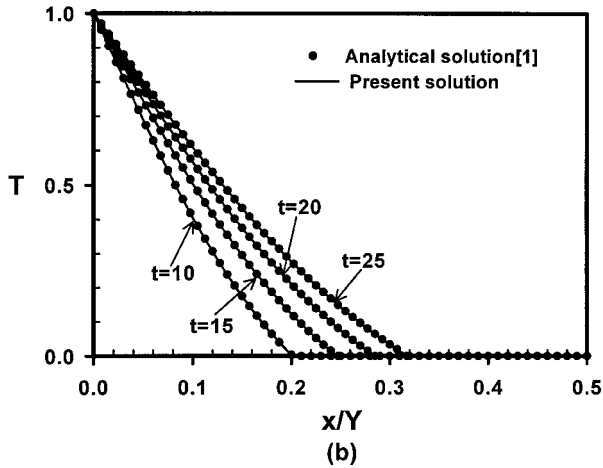

Figure 5. Panels showing the comparison between present computational solutions and analytical solutions for Example 1 (St = 2.8576). Interfacial position as a function of time and temperature distribution as a function of position at different times are shown in (*a*) and (*b*), respectively.

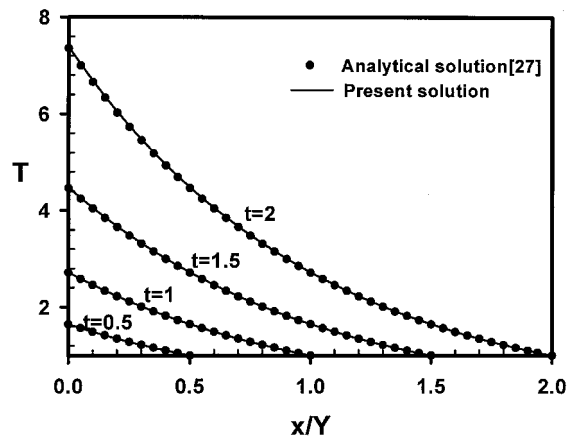

Figure 6. Diagram showing temperature distribution as a function of position at different times for Example 1.

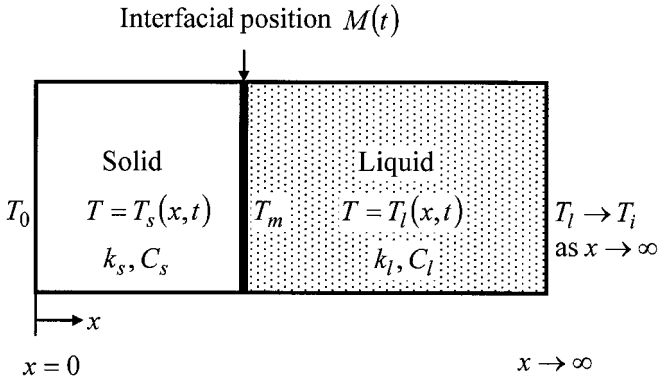

Figure 7. Schematic diagram showing the coordinate, nomenclature, boundary conditions, solid and liquid phases, and interfacial position for Example 2.

and liquid phases are given as

$$\frac{T_s(x,t) - T_0}{T_m - T_0} = \frac{\text{erf}\,\left(x/2\sqrt{\alpha_s t}\right)}{\text{erf}\,(\lambda)}$$

and

$$\frac{T_l(x,t) - T_i}{T_m - T_0} = \frac{\text{erfc}\,\left(x/2\sqrt{\alpha_l t}\right)}{\text{erfc}\,\left(\lambda\sqrt{\alpha_s/\alpha_l}\right)}$$

respectively. The parameter λ is determined from the following transcendental equation:

$$\frac{e^{-\lambda^2}}{\text{erf}\,(\lambda)} + \frac{k_l}{k_s}\left(\frac{\alpha_s}{\alpha_l}\right)^{1/2}\frac{T_m - T_i}{T_m - T_0}\,\frac{e^{-\lambda^2(\alpha_s/\alpha_l)}}{\text{erfc}\,\left(\lambda\sqrt{\alpha_s/\alpha_l}\right)} = \frac{\lambda L\sqrt{\pi}}{C_s(T_m - T_0)}$$

To simulate this problem by the LB scheme, α_s is differnt from α_l, and the relaxation times, τ, were set to be different values for the separated liquid and solid phases. For those lattices occupied by both phases, the relaxation time was determined according to the following expression:

$$\tau = \frac{1}{2} + \frac{\alpha_l}{\alpha_s}\left(\tau_s - \frac{1}{2}\right) f_l$$

where τ_s is the relaxation time corresponding to the solid diffusivity α_s. The dependence of temperature distribution on the diffusitivty ratio, α_l/α_s, as a function of x^* at $t^* = 1$ is shown in Figure 8. There were 800 uniform lattices in the computational range from $x^* = 0$ to 8. The required parameters were set as follows: $\Delta x = 0.01$, $\alpha_s = 0.005$, $L = 0.5$, $\text{St} = C(T_m - T_0)/L = 2$, $C = 1$. The dimensionless time and position in this figure were defined as $x^* = x/Y$ and $t^* = \alpha_s t/Y^2$, and the numerical value of Y was set to be unity. It is shown that our results agree very well with analytical solutions. The maximum relative numerical error was less than 0.5%.

Example 3. Solidification in a Half-Space (Three-Region Problem)

A more critical test was the half-space solidification for a material exhibiting phase change over a range of temperatures rather than at a single discrete temperature value. The range for phase change is usually referred as the mushy zone. This is a three-region problem because temperatures and thermal properties are usually different in the solid phase, mushy zone, and liquid phase.

The physical problem to be simulated is described as follows. Initially a liquid phase at a uniform temeprature T_i was confined to the half-space $x > 0$. At time $t = 0$, the temperature of the boundary surface at $x = 0$ was lowered to some temperature T_0 which was below the phase-change temperature, and maintained at that temperature for all times $t > 0$. Solidification began at the surface $x = 0$ and proceeded into the material as the solid/mushy and mushy/liquid interfaces moved in the positive x direction. Figure 9 presents the coordinates, nomenclatures, and the three regions of this problem schematically.

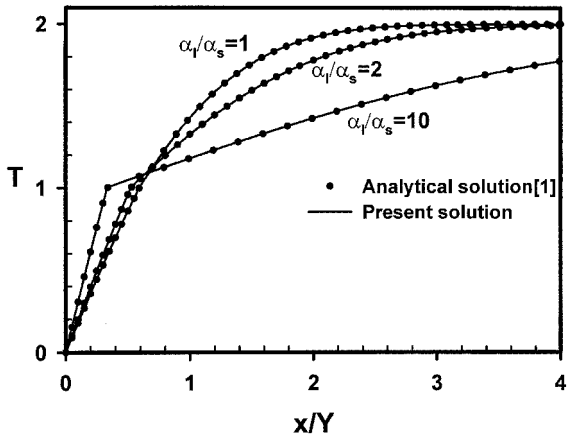

Figure 8. Diagram showing temperature distribution as functions of position and thermal diffusivity ratio at $t^* = 1$ for Example 2.

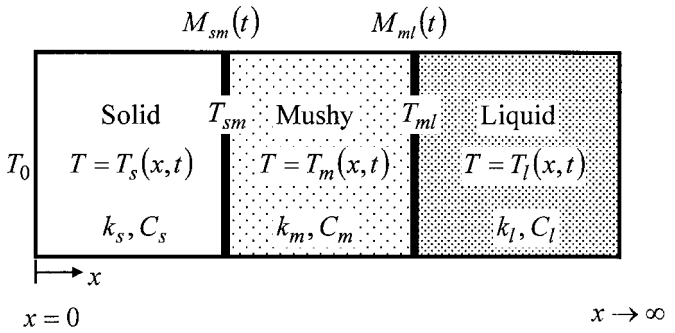

Figure 9. Schematic diagram showing the coordinate, nomenclature, boundary conditions, solid phase, mushy zone and liquid phase, and interfacial position for Example 3.

In order to make a comparison with analytical solution obtained by Cho and Sunderland [2], material properties were assumed to be constant in every single phase, and the material properties were specified as $k_l/k_s = 0.6$, $k_m/k_s = 0.76$, $C_l/C_s = 1.2$, and $C_m/C_s = 1.12$, where k and C individually represent the thermal conductivity and heat capacity, while the subscripts *s, m, l* refer to the solid phase, mushy zone, and liquid phase, respectively. The dimensionless temperature was defined as $T^* = (T - T_0)/(T_i - T_0)$. The interfacial temperatures at the solid/mushy and mush/liquid were set at 0.6 and 0.8, respectively.

The temperature distribution as a function of position at time $t^* = 1$ ($t^* \equiv \alpha_s t/Y^2$) for two Stefan numbers, $\mathrm{St} = 0.1$ and 1.0 [$\mathrm{St} \equiv C_s(T_i - T_0)/L$], are presented in Figure 10*a*. The solid/mushy and mushy;/liquid interfacial positions as a function of time are shown in Figure 10*b*. There were 500 lattices uniformly distributed in the computational range from $x^* = 0$ to 5 for this case. As can be seen in Figure 10, excellent agreement between our solutions and the analytical solutions was achieved. The steplike behavior of the solution, appearing in Figure 10*b*, was the numerical error due to the enthalpy formulation, which can be reduced by increasing the cell numbers or by using a suitable weighting-function scheme [9]. It is noted that the temperture profile, in Figure 10*a*, presents a steeper slope in the mushy zone for $\mathrm{St} = 0.1$ than that for $\mathrm{St} = 1$. This is because for a smaller St number, a larger amount of latent heat was released during solidification.

Example 4: Solidification from a Corner in a Quarter-Space

In this example, solidifcation of a liquid, initially at a uniform temperature T_i, which is greater than or equal to the fusion temperature T_m, confined to a two-dimensional quarter-space $x, y > 0$, was considered. At time $t = 0$, temperatures on the boundary surfaces at $x = 0$ and $y = 0$ were lowered to some fixed temperture T_0 which was below the phase-change temperature T_m, and maintained at that temperature for all times $t > 0$. Solidification began along the surfaces $x = 0$ and $y = 0$ and proceeded into the material. In order to make comparisons with the analytical solution presented by Rathjen and Jiji [3], we set $T_l = 0.3$, $T_0 = -1$, and $T_m = 0$. It was also assumed that material properties were constants. The schematic diagram showing the coordinates, nomenclatures, boundary conditions, and the two phases involved is given in Figure 11.

The interface of phase change at $t^* = 0.25$ for $\mathrm{St} = 4$, defined as $\mathrm{St} = C_s(T_m - T_0)/L$, obtained both by the LB scheme using the D2Q9 lattice and by analytical solution from [3] is presented in Figure 12. The time-step size was set at $\Delta t = 0.0025$ and the interfacial position was determined through linking locations whose liquid-phase fraction f_l was equal to 0.5. No remarkable differences between the analytical solution and the present solution can be observed from Figure 12. Due to the limitation of the analytical solution, the numerical result obtained by the hybrid numerical scheme [10] was also used for comparison. Figure 13 shows the comparison for isotherms at $t^* = 0.25$. Again, close agreement was demonstrated.

This example shows that the LB scheme can produces accurate results for two-dimensional heat conduction problems with phase change. Due to its simple computational algorithm and easy implementation of boundary conditions, the

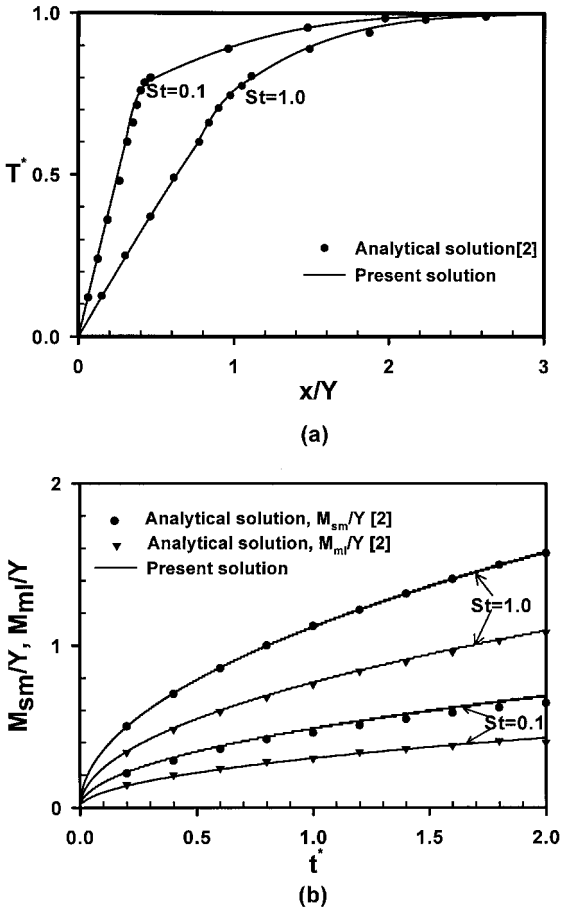

Figure 10. Panels showing the comparison between present computational solutions and analytical solutions for Example 3. (*a*) Temperature distribution as a function of position for two Stefan numbers. (*b*) Interfacial positions as a function of time at two Stefan numbers.

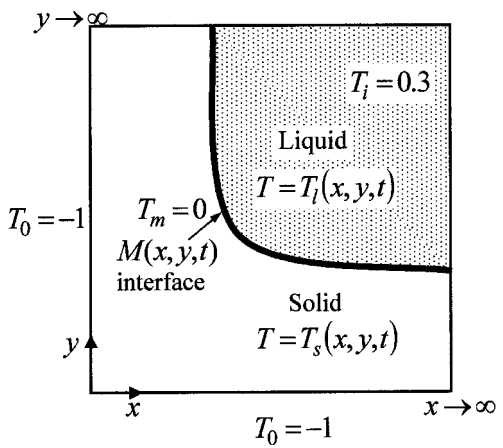

Figure 11. Schematic diagram showing the coordinates, nomenclature, initial and boundary conditions, solid and liquid phases, and interfacial position for Example 4.

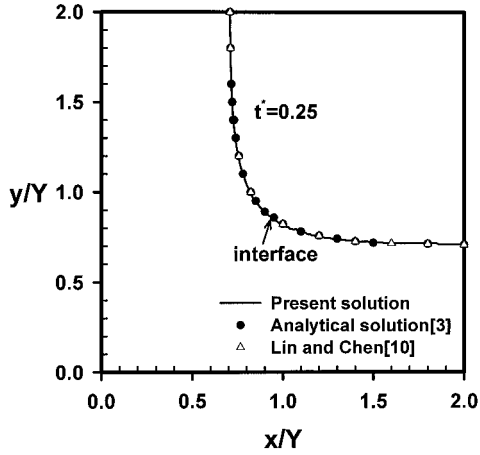

Figure 12. Diagram showing the interfacial position of phase change at $t^* = 0.25$ for Example 4.

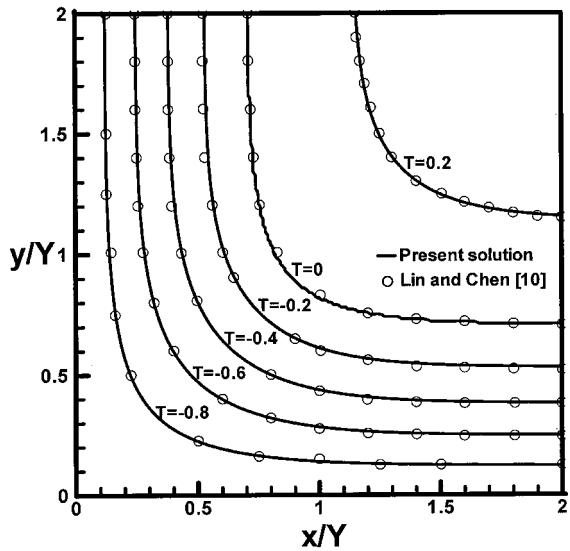

Figure 13. Diagram showing isotherms at $t^* = 0.25$ for Example 4.

LB method can be a very useful tool for two-dimensional heat conduction problems with phase change.

CONCLUSIONS

A computational scheme for the LB equation with a source term, the extended LB scheme, has been devloped for the simulation of phase-change problems governed by the heat conduction equation. The governing equation was derived through the enthalpy formulation, where the latent heat of phase change was separated from the sensible heat. The Chapman-Enskog expansion demonstrated that the proposed extended LB equation matches the governing equation

macroscopically. An appropriate numerical solution procedure for incorporating the enthalpy formation into the extended LB equation was also introduced.

Test examples including one-dimensional half-space melting and solidification as well as two-dimensional solidification in a corner were illustrated. Two types of boundary condition considered in this study were prescribed temperature and prescribed heat flux. The former was accomplished by fixing the number density on the boundary. For the latter, an algebraic equation for temperature depending on the prescribed heat flux was derived that was then executed as the case of prescribed boundary temperature. The variation of thermal diffusivities in the separated phases was realized through varying the relaxation times in the LB equation.

All numerical results obtained by the present method agree very well with analytical solutions or numerical results in the literatures. Our proposed extended LB equation can, therefore, accurately simulate both one- and two-dimensional heat conduction problems with phase change. Because of its attractive simplicity, stability, accuracy, as well as inherent parallel nature, the LB method might be a potentially powerful tool for phase-change problem with complicated boundary conditions and multiphase interfaces.

REFERENCES

1. M. N. Ozisik, *Heat Conduction*, Wiley, New York, 1980.
2. S. H. Cho and J. E. Sunderland, Heat-Conduction Problems with Melting or Freezing, *J. Heat Transfer*, vol. 91, pp. 421–426, 1969.
3. K. A. Rathjen and L. M. Jiji, Heat Conduction with Melting or Freezing in a Corner, *J. Heat Transfer*, vol. 93, pp. 101–109, 1971.
4. V. R. Voller, M. Cross, and N. C. Markatos, An Enthalpy Method for Convection/Diffusion Phase Change, *Int. J. Numer. Math. Eng.*, vol. 24, pp. 271–284, 1987.
5. W. Shyy, H. S. Udaykumar, M. M. Rao, and R. W. Smith, *Computational Fluid Dynamics with Moving Boundaries*, Taylor &amp Francis, Washington, DC, 1996.
6. R. Griffith and B. Nassersharif, Comparison of One-Dimensional Interface-Following and Enthalpy Methods for the Numerical Solution of Phase Change, *Numer. Heat Transfer B*, vol. 18, pp. 169–187, 1990.
7. Z.-X. Gong and S. Mujumdar, Noniterative Procedure for the Finite-Element Solution of the Enthalpy Model for Phase-Change Heat Conduction Problems, *Numer. Heat Transfer B*, vol. 27, pp. 437–446, 1995.
8. J.-Y. Lin and H.-T. Chen, Numerical Analysis for Phase Change Problems with the Mushy Zone, *Numer. Heat Transfer A*, vol. 27, pp. 163–177, 1995.
9. S. L. Lee and R. Y. Tzong, An Enthalpy Formulation for Phase Change Problems with a Large Thermal Diffusivity Jump across the Interface, *Int. J. Heat Mass Transfer*, vol. 34, pp. 1491–1502, 1991.
10. J.-Y. Lin and H.-T. Chen, Hybrid Numerical Scheme for Nonlinear Two-Dimensional Phase-change Problems with the Irregular Geometry, *Heat and Mass Transfer*, vol. 33, pp. 51–58, 1997.
11. G. R. McNamara and G. Zanetti, Use of the Boltzmann Equation to Simulate Lattice-Gas Automata, *Phys. Rev. Lett.*, vol. 61, pp. 2332–2335, 1988.
12. A. K. Gunstensen and D. H. Rothman, Lattice Boltzmann Model of Immiscible Fluids, *Phys. Rev. A*, vol. 43, pp. 4320–4327, 1991.

13. X. Shan and H. Chen, Lattice Boltzmann Model for Simulating Flows with Multiple Phases and Components, *Phys. Rev. E*, vol. 47, pp. 1815–1819, 1993.
14. F. J. Alexander, S. Chen, and J. D. Sterling, Lattice Boltzmann Thermodynamics, *Phys. Rev. E*, vol. 47, pp. 2249–2252, 1993.
15. X. Shan, Simulation of Rayleigh-Benard Convection Using a Lattice Boltzmann Method, *Phys. Rev. E*, vol. 55, pp. 2780–2788, 1997.
16. S. Chen and G. D. Doolen, Lattice Boltzmann Method for Fluid Flows, *Annu. Rev. Fluid Mech.*, vol. 30, pp. 329–364, 1998.
17. D. Wolf-Gladrow, *Lattice-Gas Cellular Automata and Lattice Boltzmann Models: An Introduction* , Springer-Verlag, Berlin–Heidelberg, 2000.
18. D. Wolf-Gladrow, A. Lattice Boltzmann Equation for Diffusion, *J. Stat. Phys.*, vol. 79, pp. 1023–1032, 1995.
19. G. De Fabritiis, A. Mancini, D. Mansutti, and S. Succi, *Mesoscopic Models of Liquid/Solid Phase Transitions*, *Int. J. Modern Phys. C*, vol. 9, pp. 1405–1415, 1998.
20. R. G. M. van der Sman, M. H. Ernst, and A. C. Berkenbosch, Lattice Boltzmann Scheme for Cooling of Packed Cut Flowers, *Int. J. Heat Mass Transfer*, vol. 43, pp. 577–587, 2000.
21. B. Chopard and P. O. Luthi, Lattice Boltzmann Computations and Applications to Physics, *Theor. Comput. Sci.*, vol. 217, pp. 115–130, 1999.
22. U. Frish, D. d'Humieres, B. Hasslacher, P. Lallemand, Y. Pomeau, and J.-P. Rivet, Lattice Gas Hydrodynamics in Two and Three Dimensions, *Complex Syst.*, vol. 1, pp. 649–707, 1987.
23. U. Frisch, B. Hasslacher, and Y. Pomeau, Lattice-Gas Automata for Navier-Stokes Equations, *Phys. Rev. Lett.*, vol. 56, pp. 1505–1508, 1986.
24. J. G. M. Eggels and J. A. Somers, Numerical Simulation of Free Convective Flow Using the Lattice-Boltzmann Scheme, *Int. J. Heat Fluid Flow*, vol. 16, pp. 357–364, 1995.
25. X. Shan, Simulation of Rayleigh-Benard Convection Using a Lattice Boltzmann Method, *Phys. Rev. E*, vol. 55, pp. 2780–2788, 1997.
26. S. V. Patankar, *Numerical Heat Transfer and Fluid Flow*, Hemisphere, Washington, DC, 1980.
27. R. M. Furzeland, A Comparative Study of Numerical Methods for Moving Boundary Problems, *J. Inst. Math. Appl.*, vol. 26, pp. 411–429, 1980.